Parallel Acceleration on Removal of Optical Mapping Baseline Wandering

Ilija Uzelac[1], Shahriar Iravanian[2], Flavio H Fenton[1]

[1] School of Physics, Georgia Intitute of Technology, Atlanta, GA, USA
[2] Emory University, Atlanta, GA

Abstract

Optical mapping measurements on hearts stained with fluorescent dyes is imagining method widely accepted and recognized as a tool to study complex spatial-temporal dynamics of cardiac electro-physiology. One shortcoming of the method is baseline wandering in obtained fluorescence signals as signals relevant to transmembrane potential (V_m) change and free intracellular calcium concentration ($[Ca]_i^{+2}$), the two most used dyes, are calculated as a relative signal change in respect to the fluorescence baseline. These changes are small fractional changes often smaller than 10 %. Baseline fluorescence drifts due to dye photobleaching, heart contraction/movement artifacts, and stability of the excitation light source over time. Depending on experimental instrumentation, recording duration, signal to noise levels and study aims of the optical imagining, many research groups adopted their own techniques tailored to a specific experimental data. Here we present a technique based on finite impulse response (FIR) filters with paralleled acceleration implemented on GPUs and multi-core CPU, in MATLAB.

Keywords— **Optical mapping, baseline wandering, parallel acceleration, CUDA, FIR filter, fluorescence baseline**

1. Introduction

Optical imaging with fluorescent dyes is a powerful research tool to probe the complex dynamics of cardiac electrical activity and the underlying mechanisms of arrhythmia [1–4]. Optical mapping can be performed from a single cell to whole organ, and can measure different physiological variables, especially V_m and $[Ca]_i^{+2}$. In addition, it is possible to image multiple variables simultaneously using multi-parametric imagining systems [5–7].

When a V_m dye is injected circulating through an ex-vivo heart, it binds to the cell membranes. In a similar manner, a $[Ca]_i^{+2}$ dye diffuses into cardiac cells down its concentration gradient and binds to intracellular free calcium. As the fluorescence level of V_m dyes depends on the cell membrane potential and the fluorescence level of $[Ca]_i^{+2}$ dyes depends on changes of free calcium concentration, these two important physiological parameters can be imaged with optical mapping methods using high speed cameras, suitable excitation light source, and proper excitation and emission filters.

In recent years, development in LED technologies allowed researchers to shift from traditionally used light sources, such as lasers and tungsten-halogen bulbs. Despite many advantages (including lower price), a major drawback of LEDs is instability. Due to temperature changes, LED emission spectra shifts and total intensity varies in addition to the variability of the power source, dye photo-bleaching, dye internalization, and residual cardiac contraction, which cause further degradation of the signal quality and are shared by all the light source modalities.

As the baseline drift is in the low frequency range, it is possible to filter out the majority of the drift. For example, if the pacing frequency is 2 Hz, the frequency range from DC to 2 Hz can be filtered out as it does not contain physiological relevance in most studies. In this study, we present a baseline removal method implemented with Kaiser Window FIR filter in MATLAB. We also explore using Graphics Processing Units (GPUs) for parallel processing, given the huge amount of data generated by so called restitution protocols. The simplicity of FIR filters, described with algebraic expressions, allows implementation with embedded digital signal processors (DSP).

2. Methods

2.1. Experimental Setup

To minimize the use of animals in research, experimentally obtained data in this study was ”re-used” from other optical mapping study related to development of more accurate computer simulation models to minimize the use of animals in research. Experimental setup was published in details elsewhere [7]. All experimental procedures were approved by the office of Research Integrity Assurance of Georgia Tech under IACUC #A15034 Briefly, New Zealand White rabbit hearts were Langerdorff perfused, and stained with Di-4-ANBDQPQ (JPW-6003) [8] V_m and Rhod-2 AM $[Ca]_i^{+2}$ dye. Three red LEDs (LED En-

 ISSN: 2325-887X DOI: 10.22489/CinC.2019.433

gin) coupled with OD4 660/10 nm filters (Edmund Optics) were used for V_m dye, and three green LEDs coupled with OD4 550/10 nm filters for $[Ca]_i^{+2}$ dye excitation. Operation and intensity of the LEDs were controlled by two-channel current source system PLUMBUS (Pulsed LUMinos Bimodal Uniform Source), provided by *Aleksa Tech*, switching LED lights in sync with the camera. Series of fluorescent images corresponding to V_m dye and $[Ca]_i^{+2}$ dye dynamics were obtained using a single camera (Evolve 128) in the time-multiplexing method. Fluorescence images from the anterior view (partial RV and LV) were obtained at spatial resolution of 128 x 128 pixels (full frame) at 500 fps, 16-bits, with a dual-band pass filter of 575-610 nm and 700-900 nm (Chroma) on the camera. Data was processed on a PC machine with MATLAB (R2018b): AMD 2990WX 32-core (64-Thread), 64GB RAM, X399 platform, 1000 W PSU, and with GPUs listed in Table 1.

Table 1. GPUs tested for parallel acceleration

GPU	Cuda Cores	Memory Bandwidth
GTX 970 (Maxwell)	1664	256-bit, 224 GB/s
Titan X (Pascal)	3584	384-bit, 480 GB/s
GTX 1650 (Turing)	896	128-bit, 128 GB/s

2.2. Filtering methods

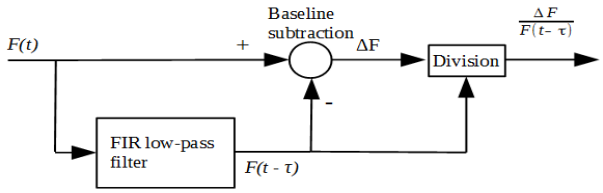

Figure 1. Baseline removal process.

In signal processing when signal distortion is not acceptable, a filter phase response needs to be a linear function of frequency (constant signal delay across all frequencies). We chose Kaiser Window filter due to its linear phase response, and the speed by which numerical filtering toolboxes compute the filter coefficients. The block schematic of the filtering method is shown on Figure 1. Conceptually, the output is a high-pass filtered version of the input signal. However, instead of directly applying a high-pass filter, a signal trace from a particular image pixel is low-pass filtered, subtracted from the original signal, and at the end divided with the baseline fluorescence (the low passed filter output) to extract the relative signal change. This way we obtain *normalized* signals, because the fluorescent signals are proportional to the excitation light intensity, which is in turn assumed to be responsible for most of the baseline drift. The low-pass FIR filter introduces delay τ , and in numerical computation it is necessary to time shift the filtered signal by the time τ prior to its subtraction from the input signal. Consequentially, portions of the output normalized signal equal to time τ at the beginning, due to filter settling time, and at the end, due to time shift, are lost. The filter delay depends on filter parameters and needs to be optimized minimizing the filter delay and signal distortion, while separating the baseline drift from the actual signal.

3. Results

The experiments were performed to find the cardiac restitution curve, i.e., the dependence of action potential duration to previous diastolic interval. For each recording, optical images were acquired for extended time, while pacing cycle length (PCL) was decreased in steps from 550 ms to 130 ms until fibrillation occurred [7]. Figure 2 shows the characteristic of V_m and Ca signals from a representative image pixel illustrating the complexity of non-linear baseline drift. It is typical for the amplitude of the V_m signals to decrease at faster pacing rates. The baseline drift is mainly related to thermal instabilities of LEDs. Figure 3 shows FFT spectra respectively. Frequency range from DC to lowest pacing rate of 1.8 Hz can be filtered out, Figure 4, as the baseline drift is a slow change in baseline fluorescence that occurs on a time scale slower than the slowest pacing period. Appearance of any peak in the frequency range from DC - 1.8 Hz reveals presence of the baseline drift.

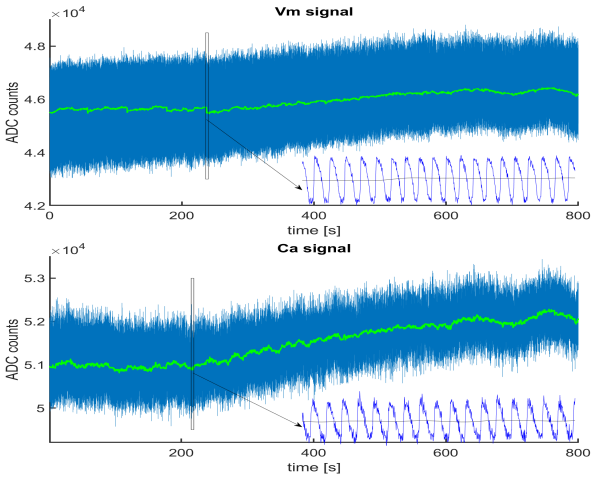

Figure 2. V_m and Ca fluorescence signals. Zoomed-in portions correspond to the intervals marked with red stripes.

While it is desirable that F_{pass} is closer to F_{cut} , steeper filter designs significantly increase the filter delay time as indicated on Figure 5, left panel. In the right panel is plotted filter delay for different flatness A_p (allowed ripple) for filter pass-band range (DC - 0.9 Hz). Computation time is directly proportional to the filter delay. To optimize the filter delay we have adopted $F_{pass}/F_{cut} = 0.5$, and $A_p = 0.1$

dB (˜1% ripple). As the amplitude of signal is usually less than 10 % of the baseline level, there is inherited attenuation of 20 dB. Therefore, filter designs need not to have over A_{st} = 40 dB attenuation in the stop band as higher attenuation leads to longer filter delays.

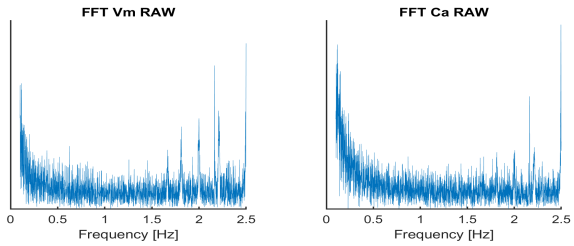

Figure 3. Frequency spectra of the V_m and Ca signals.

V_m and Ca signals from Figure 1 are shown in Figure 6 with baseline drift filtered out. For each PCL a series of 150 action potentials is recorded allowing signal stacking [9], increasing the signal-to-noise ratio with no smoothing filters needed. Stacked signals for PCL = 140 ms show presence of alternans. Figure 7 shows computational time required to process 15,000 images (60s at 250 fps) recorded at 128x128 pixels. Modern entry level GPU, GTX 1650, is on par with older architecture high end GPU (Titan X) despite having 1/4 of the cores. While MATLAB CUDA filter function is very efficiently implemented to process data in GPU memory, the CPU-GPU data transfer is a bottle-neck, adding dominant weight in the total processing time. The CPU-GPU transfer time depends on RAM memory speed. For comparison purposes, the filtering time using only CPU was measured by limiting number of parallel threads for MATLAB, and MATLAB automatically optimized the code (filter function) to run on as many as available threads. For quantitative analysis filters of different parameters are compared applied tested on the same restitution recording. For each of the 12 pacing intervals, action potential duration (APD) and calcium signal duration (CaD) maps are computed [7]. Three different filter settings are used: A_p = 1 dB, A_{st} = 20 dB; A_p = 0.1 dB, A_{st} = 20 dB; A_p = 1 dB, A_{st} = 60 dB. For all filter pairs and for each APD and CaD map, two sample t-test, assuming equal mean value was performed, $p < 0.05$ was considered statistically significant. There was no statistical difference among APDs, and CaDs values.

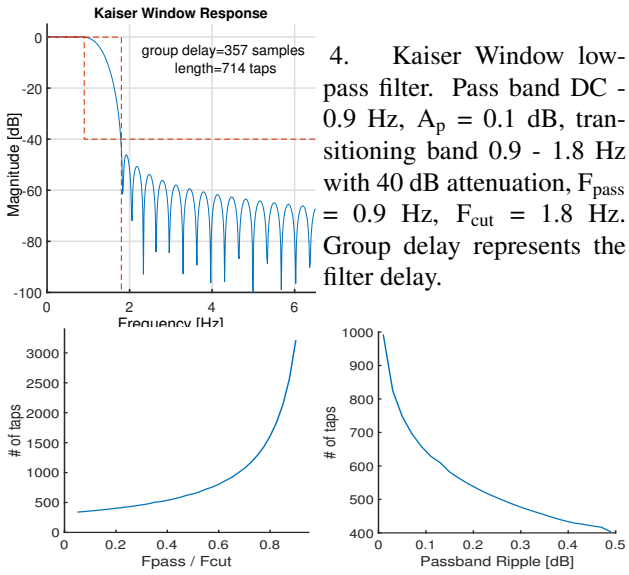

4. Kaiser Window low-pass filter. Pass band DC - 0.9 Hz, A_p = 0.1 dB, transitioning band 0.9 - 1.8 Hz with 40 dB attenuation, F_{pass} = 0.9 Hz, F_{cut} = 1.8 Hz. Group delay represents the filter delay.

Figure 5. Kaiser Window filter delays (1/2 of the number of filter taps) for different F_{pass}/F_{cut} ratios (Ap = 0.1 dB), and different pass-band ripple allowances (F_{pass}/F_{cut}). Stop-band attenuation 40 dB, sampling = 250 Hz. While delay increases with faster sampling rates, shape of the curves remains the same.

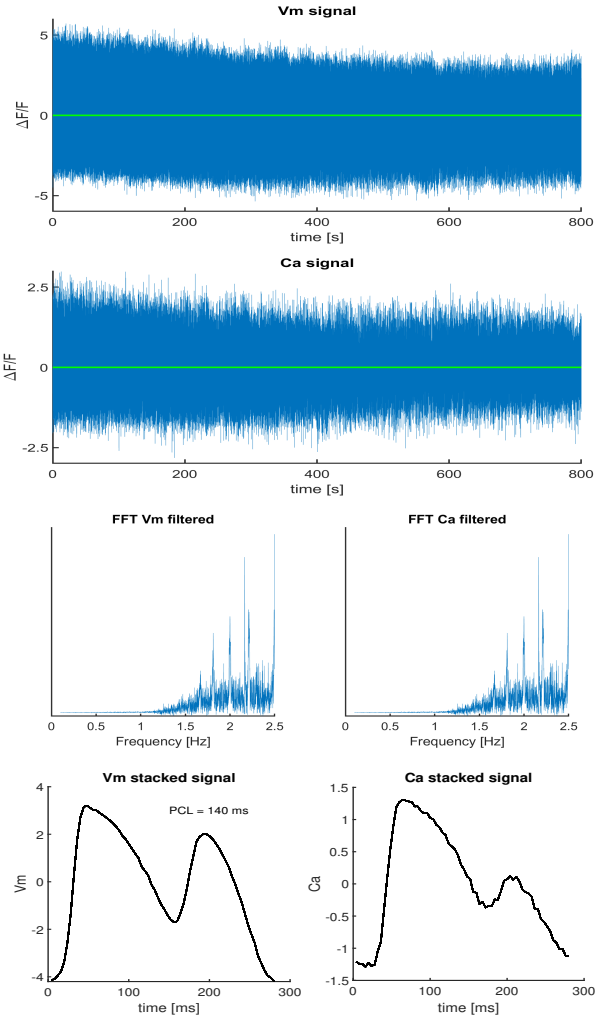

Figure 6. Filtered V_m and Ca signal, FFT spectra, and example of stacked signals for PCL = 140 ms (7.14 Hz)

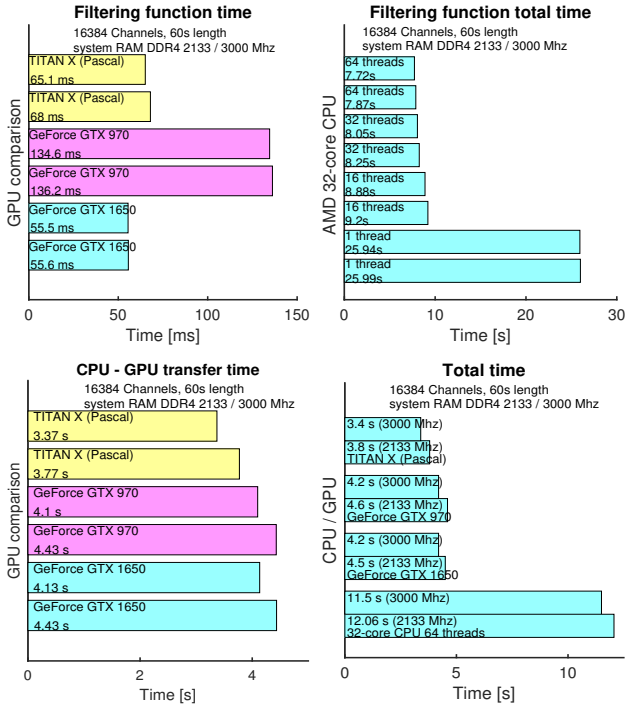

Figure 7. All GPU timing with data in GPU memory. (Upper Left) MATLAB filter function processing time. (Lower Left) CPU-GPU transfer timing forth and back including memory allocation time for all the variables including baseline and the filtered signal copied back to RAM. (Upper Right) Total processing time on CPU.(Lower Right) Comparison of total processing time on GPUs and CPU.

4. Discussion

Baseline drift removal is a first step in the processing of optical mapping data. For short time recordings, on the scale of seconds, baseline drift can be considered linear. In contrast, the baseline drift tends to be highly non-linear for long term recordings. The presented fluorescence baseline filtering methods is robust, and the filter cut-off and stop band frequency can be adjusted to the known PCL to achieve the optimal filtering. While necessary data trimming due to the filter delay is not a major issue, filters with longer delays are more computationally expensive. It is important to note if alternans are present, periodicity is not the PCL, but 1/2*PCL, and the filter cut-off frequency needs to be adjusted to 1/2*PCL or otherwise alternans would not be visible after the filtering.

5. Conclusions

In this study, we presented a robust method for fluorescence baseline removal which can be used as a first step in optical mapping signals processing pipeline. In the filter design process, only a cut-off frequency is independent while the rest of the filter parameters are optimized as shown in results section. Kaiser window filters can be implemented in DSP embedded system and systems based on microcontrollers depending on the actual application. For off-line data processing, software packages such as MATLAB are ideally suited where GPU computation toolbox can be used to speed up processing with parallel acceleration.

This work is supported with NSF CNS1446675 and NIH 1R01HL143450-01 grants.

References

[1] Pertsov AM, Davidenko JM, Salomonsz R, Baxter WT, Jalife J. Spiral waves of excitation underlie reentrant activity in isolated cardiac muscle. Circulation research 1993;72(3):631–650.

[2] Efimov IR, Nikolski VP, Salama G. Optical imaging of the heart. Circulation research 2004;95(1):21–33.

[3] Cherry EM, Fenton FH. Visualization of spiral and scroll waves in simulated and experimental cardiac tissue. New Journal of Physics 2008;10(12):125016.

[4] Fenton FH, Luther S, Cherry EM, Otani NF, Krinsky V, Pumir A, Bodenschatz E, Gilmour Jr RF. Termination of atrial fibrillation using pulsed low-energy far-field stimulation. Circulation 2009;120(6):467.

[5] Holcomb MR, Woods MC, Uzelac I, Wikswo JP, Gilligan JM, Sidorov VY. The potential of dual camera systems for multimodal imaging of cardiac electrophysiology and metabolism. Experimental biology and medicine 2009; 234(11):1355–1373.

[6] Scull JA, McSpadden LC, Himel HD, Badie N, Bursac N. Single-detector simultaneous optical mapping of v m and [ca 2+] i in cardiac monolayers. Annals of biomedical engineering 2012;40(5):1006–1017.

[7] Uzelac I, Ji YC, Hornung D, Schröder-Scheteling J, Luther S, Gray RA, Cherry EM, Fenton FH. Simultaneous quantification of spatially discordant alternans in voltage and intracellular calcium in langendorff-perfused rabbit hearts and inconsistencies with models of cardiac action potentials and ca transients. Frontiers in physiology 2017;8:819.

[8] Matiukas A, Mitrea BG, Qin M, Pertsov AM, Shvedko AG, Warren MD, Zaitsev AV, Wuskell JP, Watras J, Loew LM, et al. Near-infrared voltage-sensitive fluorescent dyes optimized for optical mapping in blood-perfused myocardium. Heart rhythm 2007;4(11):1441–1451.

[9] Uzelac I, Fenton FH. Robust framework for quantitative analysis of optical mapping signals without filtering. In 2015 Computing in Cardiology Conference (CinC). IEEE, 2015; 461–464.

Address for correspondence:

Ilija Uzelac, uzelaci@gmail.com
837 State St, School of Physics, Atlanta, GA, 30332, USA